Free Radical Biology and Medicine 188 (2022) 105–116

Contents lists available at ScienceDirect

Free Radical Biology and Medicine

journal homepage: www.elsevier.com/locate/freeradbiomed

Original article

The role of cycloastragenol at the intersection of NRF2/ARE, telomerase, and proteasome activity

Sinem Yilmaz [a,b], Erdal Bedir [c,*], Petek Ballar Kirmizibayrak [d,*]

[a] Department of Biotechnology, Graduate School of Natural and Applied Sciences, Ege University, Bornova, Izmir, Turkey
[b] Department of Bioengineering, Faculty of Engineering, University of Alanya Aladdin Keykubat, Antalya, Turkey
[c] Department of Bioengineering, Izmir Institute of Technology, 35430, Urla, Izmir, Turkey
[d] Department of Biochemistry, Faculty of Pharmacy, Ege University, 35100, Bornova, Izmir, Turkey

ARTICLE INFO

Keywords:
NRF2
Telomerase
Proteasome
Aging
Cycloastragenol
Oxidative stress
Neuroprotection

ABSTRACT

Aging is well-characterized by the gradual decline of cellular functionality. As redox balance, proteostasis, and telomerase systems have been found to be associated with aging and age-related diseases, targeting these systems with small compounds has been considered a promising therapeutic approach. Cycloastragenol (CA), a small molecule telomerase activator obtained from *Astragalus* species, has been reported to positively affect several age-related pathophysiologies, but the mechanisms underlying CA activity have yet to be reported. Here, we presented that CA increased NRF2 nuclear localization and activity leading to upregulation of cytoprotective enzymes and attenuation of oxidative stress-induced ROS levels. Furthermore, CA-mediated induction of telomerase activity was found to be regulated by NRF2. CA not only increased the expression of hTERT but also its nuclear localization *via* upregulating the Hsp90-chaperon complex. In addition to modulating nuclear hTERT levels at unstressed conditions, CA alleviated oxidative stress-induced mitochondrial hTERT levels while increasing nuclear hTERT levels. Concomitantly, H_2O_2-induced mitochondrial ROS level was found to be significantly decreased by CA administration. Our data also revealed that CA strongly enhanced proteasome activity and assembly. More importantly, the proteasome activator effect of CA is dependent on the induction of telomerase activity, which is mediated by NRF2 system. In conclusion, our results not only revealed the cross-talk among NRF2, telomerase, and proteasome systems but also that CA functions at the intersection of these three major aging-related cellular pathways.

1. Introduction

Aging is associated with a general decrease in cellular functionality. Several hallmarks such as genomic instability, telomere attrition, epigenetic alterations, decline of proteolysis, mitochondrial dysfunction, cellular senescence, stem cell exhaustion, and altered intercellular communication have been described for aging cells [1]. These changes not only lead to an acceleration of the progression of aging but also to the development of age-related pathologies such as cardiovascular diseases, diabetes, and neurodegenerative diseases. Telomere shortening, increased reactive oxygen species (ROS) formation, and decline of proteasomal activity are three main conserved cellular alterations upon aging that have been a focus of research to promote healthier aging [1].

The accumulation of oxidative damage is one of the critical factors during aging, and its alleviation has been shown to extend the lifespan [2]. The NRF2 (nuclear factor erythroid 2–related factor 2)/KEAP1 (Kelch-like ECH-associated protein 1) signaling pathway is a major cellular defense mechanism against oxidative stress [2]. While NRF2 is a redox sensing transcription factor and coordinates many cytoprotective genes, mainly including Antioxidant Response Elements (AREs) promoter region [3,4], KEAP1 is the negative regulator of this signaling pathway, and its function depends on the intracellular redox state [5]. Under unstressed conditions, KEAP1 sequesters NRF2 in the cytoplasm and promotes its ubiquitination and proteasomal degradation. Increased oxidative stress induces a conformational change in the NRF2-KEAP1 complex preventing the ubiquitination of NRF2 and promoting its nuclear translocation [6]. It is well known that NRF2 inactivation exacerbates the progression of several aging-related phenotypes and dysfunctions [7–14]. As several studies describe that NRF2 activity is decreased upon aging, and enhanced NRF2 activity correlates with extended lifespan in various organisms, NRF2 has been implicated as a

* Corresponding authors.
E-mail addresses: erdalbedir@iyte.edu.tr (E. Bedir), petek.ballar@ege.edu.tr (P. Ballar Kirmizibayrak).

https://doi.org/10.1016/j.freeradbiomed.2022.06.230
Received 2 June 2022; Received in revised form 9 June 2022; Accepted 14 June 2022
Available online 17 June 2022

Abbreviations

NRF2	nuclear factor erythroid 2–related factor 2
KEAP1	Kelch-like ECH-associated protein 1
ARE	Antioxidant Response Elements
TERT	telomerase reverse transcriptase
TERC	Telomerase RNA Component
CA	Cycloastragenol
DMF	Dimethyl fumarate
18α-GA	18α-Glycyrrhetinic acid
6-OHDA	6-hydroxydopamine
GA	geldanamycin
DTT	dithiothreitol
H_2DCFDA	2′-7′- Dichlorodihydrofluorescein diacetate
ROS	reactive oxygen species
H_2O_2	hydrogen peroxide
HO-1	heme oxygenase 1
GR	glutathione reductase
GCLC	glutamate-cysteine ligase catalytic subunit
CHIP	C terminus of Hsc70-interacting protein
Hsp90	Heat shock protein 90
FKBP52	FK506-binding protein 52
HEKn	neonatal human primary epidermal keratinocytes
IB	immunoblotting
IP	immunoprecipitation

therapeutic target in age-related diseases [15].

The ability of the cell to maintain its protein homeostasis (proteostasis) is also affected upon aging progression. The proteasome, a multicatalytic enzyme complex located in the cytosol and nucleus, is formed by the assembly of the barrel-shaped proteolytic core particle (20 S) and the regulatory particle (19 S) [16]. Proteasome, which is considered as the main component for surveilling proteostasis, is responsible for degradation of misfolded, unfolded, damaged, short-lived, or regulatory proteins, which are modified by a poly-ubiquitin chain that facilitates their recognition by the proteasome. In addition to ubiquitin-dependent proteasomal degradation, certain fractions of unfolded and intrinsically disordered proteins are also degraded by proteasome in a ubiquitin-independent manner, especially under oxidative stress [17,18]. The activity of the proteasome decreases dramatically with aging [19,20]. The accompanied progressive accumulation of damaged or misfolded proteins by proteasomal dysfunction is increased to lead to aging and/or age-related diseases. Hence, the inhibition of proteasome in young cells induced premature senescence-like phenotype [21]. Downregulation of proteasome subunit expressions, alterations in post-translational modification of subunits, disruption of proteasome assembly, and occlusion of the proteasome by aggregated or cross-linked proteins are reported factors responsible for the reduction of proteasome activity observed during the aging process [22,23]. Thus, several approaches to enhance proteasome activity such as genetic manipulations, post-translational modifications and small molecule proteasome agonists have been depicted to prevent or decelerate the progression of age-related diseases such as Parkinson's and Alzheimer's and extend health span and longevity [20,22,24,25].

Telomeres, consisting of TTAGGG repeats, are located at the ends of linear chromosomes and become progressively shorter upon each cell division [26]. Telomerase, which contains a telomerase reverse transcriptase (TERT) and the Telomerase RNA Component (TERC), reverse transcribes telomeres and retards cellular aging [27]. TERT expression and telomerase activity are very low or absent in most multicellular eukaryotic organisms but are significantly high in stem cells and germ cells. Furthermore, recently it has been depicted that TERT is also present in tissues with low replicative potential, such as the heart [28,29] and the brain [30,31]. Continuingly, non-canonical functions of TERT have been very recently described, including signal transduction, gene expression regulation, protection against oxidative damage, and chaperone activity for the 26S proteasome assembly that are independent of its telomere elongation activity [32]. Considering its telomere-dependent and independent roles of TERT, its activation with potent compounds is important for developing new strategies in age-related diseases.

Cycloastragenol (CA; 20(R),24(S)-epoxy-3β,6α,16β,25-tetrahydroxycycloartane) is a small molecule telomerase activator derived from the extract of *Astragalus membranaceous*, a plant commonly used in traditional Chinese medicine to treat several diseases such as diabetes, hyperlipidemia, atherosclerosis, and cancer. CA not only increases telomerase activity and elongates telomere length but also extends life span of mice without augmenting cancer incidences [33]. Additionally, CA (or CA-containing TA-65®) has been shown to have beneficial effects on several conditions such as glucose intolerance, insulin resistance, immunity, neural depression, age-related macular degeneration, and cardiovascular diseases [34–39]. Furthermore, several clinical studies suggest that, as a new dietary supplement, TA-65® may enhance one's health span without any adverse effects [34]. Despite all the promising effects of CA, which were demonstrated by several studies, the underlying molecular mechanisms of how CA affected telomerase and redox balance were missing. In this study, we report for the first time that proteasome activator action of CA is dependent on induction of telomerase activity, which is driven by activation of NRF2 system. In conclusion, our results not only revealed the cross-talk among NRF2, telomerase, and proteasome systems but also that CA functions at the intersection of these three major aging-related cellular pathways.

2. Materials and methods

2.1. Reagents and antibodies

While DMF (Dimethyl fumarate) (242926), 18α-GA (18α-Glycyrrhetinic acid) (G8503), 6-OHDA (6-hydroxydopamine) (H4381), and DMSO (Dimethylsulfoxide; D2650) were purchased from Sigma Aldrich, GA (geldanamycin) (13355) was obtained from Cayman Chemical, and Mg-132 (474790) was obtained from Calbiochem. The proteasome fluorogenic substrates [Suc-LLVY-AMC-BML-P802-0005 for the ChT-L (chymotrypsin-like), Z-LLE-AMC-BML-ZW9345-0005 for the C-L (caspase-like), and Boc-LRR-AMC-BML-BW8515 for the T-L (trypsin-like)] and primary proteasome antibodies against β1 (BML-PW8140), β2 (BML-PW8145), β5 (BML-PW8895), α4 (BML-PW8120), and α6 (BML-PW8100) were purchased from Enzo Life Sciences. Antibodies against NRF2 (Abcam, Ab-62352), NRF2 (Bioss, bsm-52179R), hTERT (Origene, TA301588), KEAP1 (CST-8047), HO-1 (CST-5853), Hsp90 (Santa Cruz, sc-69703), p23 (Santa Cruz, sc-101496), CHIP (Santa Cruz, sc-133066), FKBP52 (Santa Cruz, sc-100758) and p16 (CST, 80772) were used in this study. Antibodies against β-actin (Sigma-Aldrich-A5316), GAPDH (CST, 5174), α-Tubulin (CST, 3873), VDAC (CST, 4661), and Lamin A-C (CST, 4777) were used as loading control. Secondary antibodies (Goat anti-rabbit-31460 and Goat anti-mouse-31430) were purchased from Thermo Fisher Scientific.

2.2. Cell line and culture conditions

HEKn (human neonatal epithelial keratinocyte cells) cells were obtained from the American Type Culture Collection (ATCC; PCS-200-010) and cultured in Dermal Cell Basal Media (ATCC; PCS-200-030) supplemented with Keratinocyte Growth Kit (ATCC; PCS-200-040) according

to supplier's instructions at 37 °C under humidified 5% CO_2. HEKn cells were sub-cultured when they reached 70–80% confluency.

SHSY-5Y (human neuroblastoma) cells were obtained from the American Type Culture Collection (ATCC; CRL-2266) and cultured in DMEM (Dulbecco's modified Eagle's medium; Lonza, BE12-604F) supplemented with 10% FBS (fetal bovine serum, Biological Ind., Israel, 04-007-1A) and 2 mM L-glutamine (Biological Ind., Israel, 03-020-1B) at 37 °C under humidified 5% CO_2.

2.3. Cellular fractionation

HEKn cells were treated with indicated doses of CA or DMSO for 24 h. Nuclear-cytoplasmic fractionation was performed according to the NE-PER kit (Pierce, Thermo Fisher Scientific, US, 78833). The cytosolic and nuclear fractions were analyzed by immunoblotting for the nuclear translocation of both NRF2 and hTERT. In these experiments, GAPDH and α-Tubulin were used as cytoplasmic loading controls and Lamin A-C as a nuclear loading control.

Mitochondrial and nuclear cellular fractions were performed *via* Mitochondrial Isolation Kit (Thermo Fisher Scientific, US, 89874), as previously reported [40]. Briefly, the cells were lysed in lysis buffer, then centrifuged at 800 g for 10 min. After centrifugation and washing steps with 1x PBS, the nuclear pellet was lysed in 1% Nonidet P-40, 0.5% sodium deoxycholate, and 0.1% SDS in 1X PBS, pH 8.0 and centrifuged at higher speed as 16,000xg for 20 min. The supernatant containing mitochondrial and cytoplasmic fractions was centrifuged at higher speed as 12,000xg for 10 min. The pellet was dissolved in 1% Nonidet P-40, 0.5% sodium deoxycholate, and 0.1% SDS in 1X PBS, pH 8.0, and centrifuged to obtain soluble mitochondrial protein. After performing cellular fractionation, nuclear and mitochondrial protein levels were determined by BCA protein assay (Thermo Fisher Scientific, US, 23, 225). In these experiments, while VDAC was used as a mitochondrial loading control, Lamin A-C was used as a nuclear loading control.

2.4. Immunofluorescence analysis

HEKn cells were seeded on 6 well plate with coverslips for fluorescence microscopy [41]. The next day, cells were treated with the indicated concentration of CA for 24 h. Then, cells on coverslips were washed twice with cold 1X PBS and fixed with 4% paraformaldehyde in PBS for 30 min at 4 °C. After washing six times with PBS, cells were blocked with 0.01% saponin and 0.01% BSA in PBS for cell permeabilization. The samples were first incubated with anti-NRF2 antibody (Abcam, Ab-62352, 1:250 dilution) at 4 °C overnight and then with Alexa Flour secondary antibody (Pierce, A-11008, 1:500 dilution) for 1 h at 37 °C. Slides were mounted *via* mounting media with DAPI (Invitrogen, P36965) for nuclei staining. Images were taken by fluorescence microscopy (Olympus IX70, Japan).

2.5. Luciferase activity assay

HEKn cells were transfected with pGL4.37[luc2P/ARE/Hygro] Vector (Promega, US, E364A) using Turbofect transfection reagent (Thermo Fisher Scientific, US, R0532) for 24 h followed by treatment of indicated concentrations of CA for 24 h. DMF (50 μM) was used as an experimental control. Cells were harvested and lysed in Cell Culture Lysis Reagent (Promega, US, E1500), and supernatants were used for luciferase activity assay according to the manufacturer's instruction. Standard deviations and means were obtained from three independent biological replicates.

2.6. Enzyme-linked immunosorbent assay (ELISA)

HEKn cells were treated with indicated doses of CA or DMSO for 24 h. Nuclear lysates were subjected to the NRF2 Transcription Factor Assay (Colorimetric, Cayman Chemical, US, 600590), which utilizes immobilized specific double-stranded DNA sequence containing the NRF2 consensus binding site, allowing investigation of the levels of nuclear NRF2 protein bound to its target DNA. The assay was performed following the manufacturer's instructions to detect nuclear NRF2 protein levels. The absorbance was read at 450 nm and obtained data was normalized to nuclear protein levels and presented as fold change compared to control cells treated with DMSO.

HO-1 (heme oxygenase 1), GCLC (glutamate-cysteine ligase catalytic subunit), and GR (glutathione reductase) protein levels were determined by ELISA kits according to the manufacturers' instructions (ABCAM ab207621, ABCAM ab233632, and Cayman Chemical 703202, respectively).

2.7. Proteasome activity assays

ChT-L, C-L, and T-L activities were assayed in crude extracts incubated with CA for 1 h or lysates obtained from cells were incubated with CA for 24 h under culture conditions as described previously. To determine proteasome subunit activities of CA, cells were lysed (with a buffer containing 8,56 g sucrose, 0.6 g HEPES, 0.2 g $MgCl_2$, 0.037 g EDTA in ml; DTT (dithiothreitol) was added freshly at a final concentration of 1 mM [42]. The supernatant was incubated with reaction mixture containing 7.5 mM MgOAc, 7.5 mM, $MgCl_2$, 45 mM KCl, and 1 mM DTT for 10 min [42] and then with fluorogenic substrates Suc-LLVY-AMC (Enzo Life Sciences, BML-P802-0005), Z-LLE-AMC (Enzo Life Sciences, BML-ZW9345-0050), and Boc-LRR-AMC (Enzo Life Sciences, BML-BW8515-0005) for 1 h to determine proteasome subunit activities. The measurements were performed by a fluorescent reader at 360 nm excitation/460 nm emission (Varioscan, Thermo Fisher Scientific, US). While DMSO was used as a solvent control, Mg-132, known as a proteasome inhibitor, was used as an experimental control. Protein concentrations were determined using the BCA (bicinchoninic acid) assay (Thermo Fisher Scientific, USA).

2.8. Measurement of cellular and mitochondrial ROS

To detect cellular ROS formation, 2′-7′-Dichlorodihydrofluorescein diacetate (H_2DCFDA) (Enzo; ALX-610-022-M050) was used as previously reported [43]. For this purpose, HEKn cells were pre-treated with indicated concentrations of CA for 1 h. After 1 h pre-treatment of CA, cells were treated with 250 μM H_2O_2 (hydrogen peroxide) for 24 h H_2DCFDA resuspended in 1X PBS at a final concentration of 10 μM was added to the cells and incubated at 37 °C for 30 min [25]. After the incubation period, half of the cells were suspended, and execution/emission absorption of the oxidative product was measured at 495 and 520 nm. The other half of cell suspension was used to determine protein concentration by BCA assay to perform normalization of absorbance. This experiment was performed in three independent experiments.

To determine mitochondrial ROS formation, MitoSOX reagent (Invitrogen™, 36008) was used as previously reported [44]. In briefly, HEKn cells were pre-treated with indicated concentration of CA for 1 h then treated with 250 μM H_2O_2 for 24 h. For fluorometric assay, HEKn cells were incubated with 5 μM concentration of MitoSOX for 15 min at 37 °C. Absorbance values (Ex:510 nm; Em:580 nm) were measured with a microplate reader (Varioskan, Thermo Fisher Scientific, USA). The obtained MitoSOX fluorescence intensity was normalized with DAPI signal (cell number). Experiments were done in triplicates.

2.9. Immunoblotting (IB)

Cell lysates were prepared in RIPA buffer (1% Nonidet P-40, 0.5% sodium deoxycholate, and 0.1% SDS in 1X PBS, pH 8.0). With protease inhibitors (Roche, Switzerland). Protein concentrations were determined by BCA assay (Thermo Fisher Scientific, US). Equal amounts of samples were loaded to the gels and separated by SDS-PAGE electrophoresis after 5-min treatment with 4X Laemmli buffer at 95°. Then, gels

were transferred to the PVDF membrane (EMD Millipore, US, IPVH00010). Membranes were blocked with 5% non-fat dry milk prepared in 1X PBS-0.1% Tween-20, then incubated with primary and secondary antibodies. β-Actin and GAPDH were used as loading control for whole lysate experiments. Chemiluminescence signals of the proteins were detected with Clarity ECL substrate solution (BIORAD, US, 1705061) by Vilber Loumart FX-7 (Thermo Fisher Scientific, US). The quantifications and analysis of proteins were determined by ImageJ software (http://imagej.nih. gov/ij/). All IB experiments were performed at least in three independent replicates.

2.10. Real-time PCR analysis

RNA isolations were performed by using Aurum Total RNA Mini Kit (Bio-Rad, USA, 7326820) according to the supplier's instructions. RNA concentrations were measured by using Beckman Coulter Du730 instrument. 1 μg RNA of each sample was used for cDNA synthesis. cDNA synthesis was performed *via* Iscript cDNA Synthesis Kit (Bio-Rad, USA, 1708891). Gene expression analysis was performed by using SYBR Green 1 (Bio-Rad, USA, 1725121) and LightCycler480 Thermocycler (Roche, Switzerland). For RT-PCR studies, specific primers against NRF2, hTERT, β1, and β5 (Supplemental Table S1). While 300 nM primer pairs of NRF2, β1, and β5 were used in 10 μl reactions, 500 nM primer pairs were used for hTERT. Fold changes of the transcripts were done by the normalizations against housekeeping gene as GAPDH. For the analysis of Ct values, Qiagen Rest 2009 program was used. Gene expression experiments were performed at three independent biological replicates with three technical replicates.

2.11. RNA interference

Specific siRNA oligo duplexes and Control siRNA (Origene, USA, SR30004) were complexed with Lipofectamine 2000 (Invitrogen, USA, 11668019) and serum-free Opti-MEM (Invitrogen, USA, 31985070) according to the manufacturer's instruction. When HEKn cells reached at confluency of 60–70%, cells were transfected with 2 and 15 nM siRNA against NRF2 (Origene, USA, SR321100) and hTERT (Origene, USA, SR322002), respectively. Equal molar control siRNA was used as experimental control. After 24 h later, media was refreshed and further incubation in complete media for HEKn cells was followed for an additional 24 h. Lastly, cells transfected with NRF2, hTERT, or control siRNA were treated with indicated doses of CA for an additional 24 h. In all silencing experiments, to ensure functional silencing of NRF2 and hTERT, the controlling of these proteins' levels was revealed by IB.

2.12. Immunoprecipitation (IP)

HEKn cells were treated with desired concentrations of CA for 24 h. Then, cells were harvested and lysed in IP buffer containing 50 mM Tris. Cl pH:8, 150 mM NaCl, 1 mM EDTA, 0.2% NP-40. Protein amounts were performed by BCA assay. 1–2 μg anti-α6 or anti-Hsp90 antibody was added to lysates with equal protein concentrations and incubated on a rotator at 4 °C overnight. Protein A-agarose beads (Invitrogen, USA, 10-1041) that were pre-washed with lysis buffer were added to lysate-antibody complexes and incubated on a rotor at 4 °C overnight. Immunoprecipitated proteins were collected by centrifugation and washed five times with Lysis Buffer and eluted from beads by boiling for 5 min in 1X Laemmlli Buffer. After IP, the samples were processed for IB.

2.13. Telomerase activity assay

The determination of telomerase enzyme activity was done in HEKn cells by using TeloTAGGG Telomerase PCR Plus Kit (Sigma Aldrich, USA, 12013789001) according to the manufacturer's instruction. Values are presented as fold change (relative value of DMSO used as a solvent control). Experiments were performed at least in three independent biological replicates.

2.14. Cell viability assay

The neuroprotective effect of CA against 6-OHDA was evaluated by MTT reagent (3-(4,5-Dimethyl-2-thiazolyl)-2,5-diphenyl-2H-tetrazolium bromide) (Sigma Aldrich, UK, M5655) according to the manufacturer's instruction. For this purpose, SHSY-5Y cells were transfected with hTERT and NRF2 specific oligo duplex (2 nM for NRF2, 15 nM for hTERT duplex) or control siRNA. After 48 h, cells were pre-treated with indicated doses of CA for 8 h. Then, cells were treated with 6-OHDA for another 16 h [45]. At the end of the incubations, the mixture of MTT and medium (1:9) was replaced with old media. The formazan crystals were dissolved in DMSO. The absorbance was measured with a microplate reader at 570 nm (Varioscan, Thermo Fisher Scientific, US) and 690 nm as a reference wavelength. Cell viability was shown as a percentage cell viability compared to cells treated with DMSO as solvent control. The MTT experiment was performed by three different replicates.

2.15. Statistical analysis

Data are exhibited as means ± standard deviation (SD). Student *t*-Test or One-way ANOVA Post Hoc test was used to analyze statistical by using GraphPad Prism software. The significance of the differences was determined as $*p \leq 0.05$, $**p \leq 0.001$, $***p \leq 0.005$.

3. Results

3.1. CA activates NRF2

The effect of CA on NRF2 signaling was first investigated *via* nuclear transcriptional activity of NRF2 in young human neonatal epithelial keratinocyte (HEKn) cells (passage 5). The treatment of CA increased both protein and mRNA levels of NRF2 in a dose-dependent manner (Fig. 1A and B). Furthermore, immunofluorescence and cellular fractionation assays revealed that CA promoted nuclear localization of NRF2 from cytoplasm (Fig. 1C and D). These observations are well-consistent with our result using the NRF2 Transcription Factor Assay, which shows a dose-dependent increase of the nuclear NRF2 protein levels (Fig. 1E). The effect of CA on the nuclear NRF2 protein levels was much more prominent in older HEKn cells at passage 15, which had entered senescence as evidenced by the expression of senescence-related p16 (Supplementary Figs. S1A and B). As our results suggest that CA might be a potent NRF2 activator, next ARE promoter activity was analyzed. Even at nanomolar concentrations, CA enhanced the relative luciferase activity more than DMF (50 μM), a well-known NRF2 activator (Fig. 1F). While CA enhanced the protein level of HO-1 (Heme oxygenase 1), one of the downstream components of NRF2 signaling, it did not significantly alter protein levels of a negative regulator, KEAP1 (Fig. 1G). We further investigated the effect of CA on the activity of the cytoprotective enzymes and found that CA increased the protein levels of HO-1, GR, and GCLC (Fig. 1H). Consistent with these results, CA treatment dose-dependently alleviated H_2O_2-induced ROS formation (Fig. 1I). Taking together, our results point out that CA treatment promotes NRF2 activation, and this activity leads to upregulation of several cytoprotective enzymes that protect cells against oxidative stress damage.

3.2. CA activates telomerase by enhancing not only hTERT expression but also its nuclear localization

Several studies have suggested that TERT mRNA expression associated with telomerase activation is elevated in response to CA treatment in primary cortical neurons, human epidermal stem cells, osteoblastic MC3T3-E1 cells, and *in vivo* in some mouse tissues [33,35,46,47]. Consistently, CA treatment promoted both hTERT protein and mRNA levels in a dose-dependent manner in young HEKn cells (Fig. 2A and B).

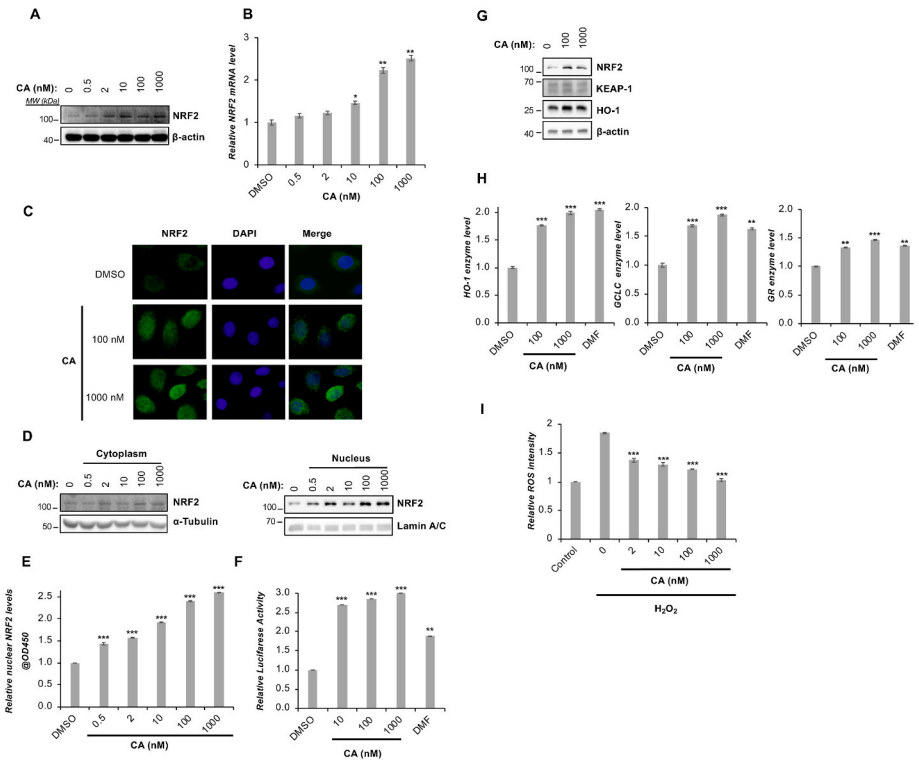

Fig. 1. The effect of CA on NRF2/ARE system. HEKn cells were treated with indicated concentrations of CA for 24 h. (A) NRF2 protein levels were determined by IB. β-actin was used as a loading control. (B) The mRNA levels of NRF2 were investigated by RT-qPCR. Error bars are presented standard error (n = 3, *p ≤ 0.05, **p ≤ 0.001, ***p ≤ 0.005). (C) The subcellular localization of NRF2 was evaluated by immunostaining using anti-NRF2 antibody. Representative fluorescent images for nuclear translocation of NRF2. DAPI was used for nuclei staining. (D) Cellular fractionation assay was performed, and NRF2 protein levels were investigated by IB. While Lamin A-C was used as nuclear loading control, α-Tubulin was used as cytoplasmic loading control. (E) NRF2 transcription factor assay using the nuclear proteins obtained from control or CA-treated cells was carried out by an ELISA kit. The obtained data was normalized to nuclear protein levels and presented as a fold change compared to control cells treated with DMSO. Error bars are presented as standard deviations ($n = 3$; *p ≤ 0.05, **p ≤ 0.001, ***p ≤ 0.005). (F) The ARE-promotor activity was determined by Luciferase activity assay. DMF (50 μM) was used as an experimental control. Error bars are presented as standard deviations (n = 3; *p ≤ 0.05, **p ≤ 0.001, ***p ≤ 0.005). (G) HO-1, KEAP1, and NRF2 protein levels were investigated by IB. β-actin was used as a loading control. (H) HO-1, GCLC and GR cytoprotective enzymes levels were quantified by ELISA. DMF (50 μM) was used as an experimental control. The protein levels were normalized to cellular total protein levels and presented as a fold change compared to control cells treated with DMSO. Error bars are presented as standard deviations ($n = 3$; *p ≤ 0.05, **p ≤ 0.001, ***p ≤ 0.005). (I) The effect of ROS (induced by H_2O_2) scavenging properties of CA was determined by H_2DCFDA. Error bars are presented as standard deviations ($n = 3$; *p ≤ 0.05, **p ≤ 0.001, ***p ≤ 0.005).

CA-mediated elevation of hTERT levels was also prominent in senescent HEKn cells (Supplementary Fig. S2). As TERT must translocate to the nucleus to form catalytically active telomerase [48], we next evaluated the localization of hTERT upon CA treatment and have found that CA enhanced hTERT translocation to the nucleus (Fig. 2C). After this observation, we further evaluated the precise molecular mechanism underlying CA-induced nuclear transport of hTERT by analyzing the effect of CA on the levels of several proteins that act as regulators of hTERT nuclear translocation. The level of CHIP (C terminus of Hsc70-interacting protein), which prevents the nuclear localization of hTERT and facilitates its degradation [49], was decreased in CA-treated HEKn cells (Fig. 2D, left, lane 2 vs. 1). The decrease in CHIP expression was also observed in senescent HEKn cells (Supplementary Fig. S3A). On the other hand, the levels of regulatory proteins Hsp90 (Heat shock protein 90), p23, and FKBP52 (FK506-binding protein 52), which function in the hTERT nuclear translocation complex, were enhanced in response to CA treatment (Fig. 2D, right, lane 2 vs. 1). Moreover, the increase in the levels of Hsp90, p23, hTERT, and FKBP52 was also observed in MRC-5 cell line (normal lung fibroblast cell line) (Supplementary Fig. S3B). As GA, a well-known Hsp90 inhibitor, was reported to inhibit telomerase activity through the ubiquitin-mediated degradation of hTERT [50], we next pre-treated cells with GA prior to CA treatment. Consistently, our results revealed that GA decreased the CA-mediated upregulation of Hsp90, p23, and FKBP52 (Fig. 2D, lane 3 vs. 2). Furthermore, GA inhibited CA-mediated nuclear translocation of hTERT as well as Hsp90-based heterocomplex (Fig. 2E). As the interaction of Hsp90 and hTERT is essential both for proper assembly of active telomerase and for nuclear import of hTERT [51–53], we next evaluated the effect of CA on the Hsp90-hTERT interaction and found that CA significantly enhanced hTERT-Hsp90 interaction (Fig. 2F).

Over the last years, non-canonical functions of hTERT have been reported, including controlling ROS levels in the cytosol and mitochondria, which is suggested to be closely related to the presence of hTERT also in mitochondria [54]. As hTERT is increased in the mitochondria upon short-term oxidative stress [54,55], the effect of CA on the mitochondrial hTERT levels was investigated. As previously reported, H_2O_2 induced the mitochondrial but not nuclear hTERT levels (Fig. 2G, lane 1 vs. 4). Our data also revealed that CA treatment increased the levels of nuclear hTERT but showed no significant change in mitochondrial hTERT levels in HEKn cells under basal conditions (Fig. 2G, lane 2 vs. 1). Furthermore, CA alleviated the H_2O_2-induced mitochondrial hTERT levels while increasing the nuclear hTERT levels decreased by H_2O_2 in HEKn cells. The effect of CA on mitochondrial ROS level induced by H_2O_2 was assessed using MitoSOX reagent. While H_2O_2 significantly increased mitochondrial ROS levels, pre-treatment of CA decreased H_2O_2-induced ROS levels (Fig. 2H). In conclusion, our results strongly suggested that CA increased not only the hTERT expression but also the levels of components of Hsp90-based heterocomplex and enhanced the nuclear localization of hTERT. Moreover, under oxidative stress, CA decreased both mitochondrial hTERT expression and mitochondrial ROS level induced by H_2O_2.

3.3. CA enhances proteasomal activity

Based on prior findings that both NRF2 and hTERT are associated with the regulation of proteasomal activity [25,56], we hypothesized that CA might activate proteasome as it enhanced NRF2 activity and hTERT levels. To verify this hypothesis, we next evaluated the effect of CA on the proteasomal activity by using fluorogenic substrates specific to each proteasome subunit. The incubation of different concentrations of CA with the proteasome-enriched lysates of HEKn did not affect the chymotrypsin-(β5), trypsin-(β2), and caspase-like (β1) activities

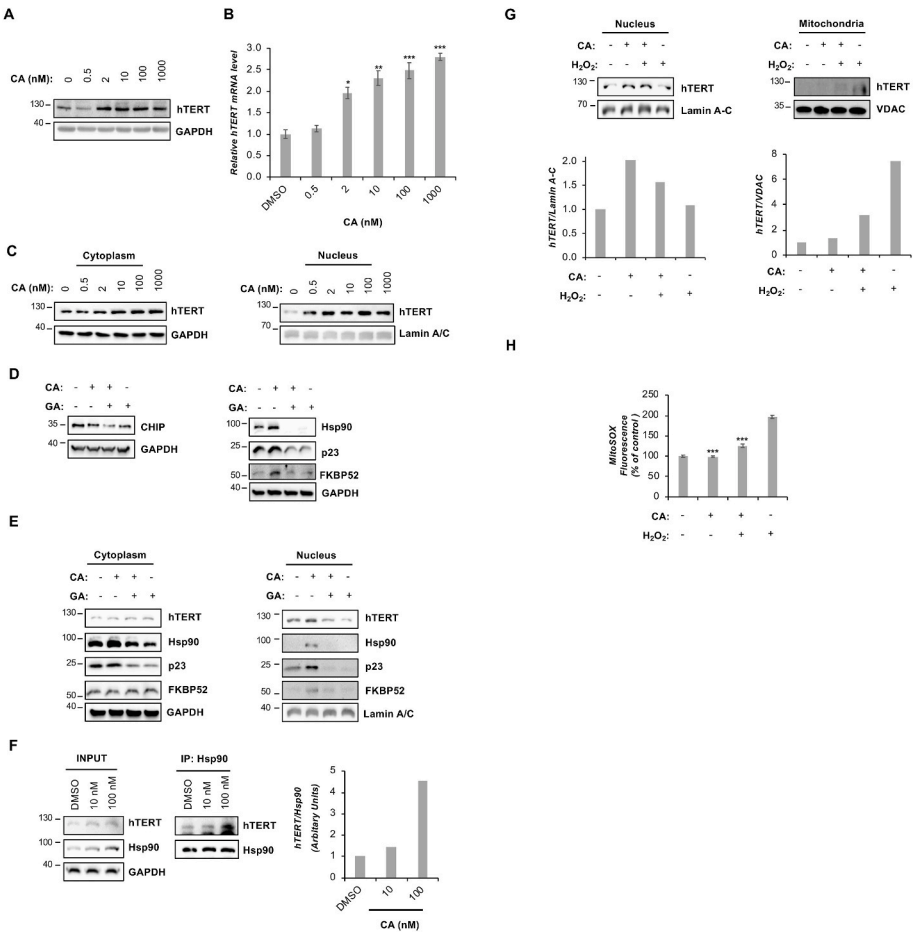

Fig. 2. CA increased not only mRNA and protein levels of hTERT but also nuclear localization of hTERT *via* Hsp90-chaperon complex. (A, B, C) HEKn cells were treated with indicated concentrations of CA for 24 h treatment. (A) The protein levels of hTERT were determined by IB. GAPDH was used as a loading control. (B) The mRNA levels of hTERT were investigated by RT-qPCR. Error bars are presented as standard deviations ($n = 3$; *p ≤ 0.05, **p ≤ 0.001, ***p ≤ 0.005). (C) The effect of CA on the hTERT nuclear localization was determined by cellular fractionation assay. hTERT protein levels were determined by IB. While Lamin A-C was used as nuclear loading control, GAPDH was used as cytoplasmic loading control. (D, E) HEKn cells were pre-treated with 100 nM GA known as Hsp90 inhibitor for 1 h, then treated with CA for an additional 24 h. (D) Total protein levels of CHIP, Hsp90, p23, and FKBP52 were determined by IB. GAPDH was used as loading control. (E) The cellular fractionation was performed and cytoplasmic and nuclear protein levels of hTERT, Hsp90, p23, and FKBP52 were determined by IB. While Lamin A-C was used as nuclear loading control, GAPDH was used as cytoplasmic loading control (F) HEKn cells were treated with indicated concentrations of CA for 24 h treatment. The effect of CA on Hsp90-hTERT association was analyzed by IP. The protein levels of Hsp90 and hTERT were evaluated by IB. GAPDH was used as a loading control for Input. (G, H) HEKn cells were pre-treated with CA for 1 h then treated with H_2O_2 for an additional 24 h. Nuclear and mitochondrial fractionation was performed. (G) Mitochondrial and nuclear hTERT levels were determined by IB. While Lamin A-C was used as nuclear loading control, VDAC was used as a mitochondrial loading control. (H) HEKn cell were incubated with MitoSOX (5 μM) for 15 min at 37 °C. Fluorometric intensity of MitoSOX was normalized by DAPI signal ($n = 3$; *p ≤ 0.05, **p ≤ 0.001, ***p ≤ 0.005).

(Fig. 3A), while proteasome inhibitor Mg-132 decreased the activity of each proteasomal subunit as expected (Supplementary Fig. S4). These observations suggested that CA did not directly target proteasomal activity. Next, HEKn cells were treated with CA for 24 h, and then the status of proteasomal activity was evaluated. While CA did not significantly affect trypsin-like activity, it significantly increased both chymotrypsin- and caspase-like activities in a dose-dependent manner (Fig. 3B). Furthermore, CA treatment increased the expression levels of β1 and β5 genes, but not β2, in a dose-dependent manner (Fig. 3C and D). Importantly, the effect of CA to increase proteasomal subunit expressions and proteasomal activity was also observed in senescent HEKn cells (Supplementary Figs. S5A and B). The analysis of proteasome assembly by proteasome IP revealed that the assembly of proteasome was enhanced following CA treatment, further demonstrating that CA induces proteasome activity (Fig. 3E). Importantly, 18α-GA, reported as a proteasome activator, enhanced proteasome assembly at micromolar concentrations [25], while CA at lower nanomolar concentrations suggesting that CA might have a better therapeutic index than 18α-GA.

3.4. NRF2 and telomerase mediated-proteasome activation by CA

Considering that CA increased the nuclear transport and activity of NRF2 and hTERT, which are associated with proteasomal activity, we next focused on the possible interrelationship of these three-biological processes in the context of CA. When NRF2 expression was silenced, the expression levels of hTERT and β1 and β5 proteasomal subunits were decreased (Fig. 4A). Interestingly, hTERT silencing had no significant effect on NRF2 levels but abolished β1 and β5 protein expression (Fig. 4A). Additionally, CA was no longer able to enhance hTERT, β1, and β5 protein levels in NRF2 silenced HEKn cells (Fig. 4B). Furthermore, NRF2 silencing completely attenuated CA-induced telomerase and proteasome activities (Fig. 4C and D). These data strongly suggest that the CA-mediated increase in telomerase and proteasome activities is driven by NRF2 activity. Interestingly, we observed that CA enhanced NRF2 protein levels but not proteasome subunit levels in hTERT silenced HEKn cells (Fig. 5A). Consistently, CA was able to enhance nuclear NRF2 protein levels, but not proteasome activity in hTERT silenced cells (Fig. 5B and C). These data suggest that the proteasome activator ability of CA is mediated by hTERT, and the enhancement of telomerase activity and hTERT levels by CA treatment is driven by NRF2 system.

3.5. CA attenuates the 6-OHDA induced toxicity via NRF2 and hTERT

In the literature, there are several studies describing CA as a neuroprotective compound against several neurotoxic agents such as Aβ1-42 peptide [57] and 6-OHDA [58]. As our data clearly revealed that CA increased NRF2, telomerase, and proteasome activity, which reportedly alleviate neurotoxicity, CA-mediated protection against 6-OHDA was next investigated in the context of the involvement of NRF2 and hTERT. To this end, control, NRF2, or hTERT-silenced SH-SY5Y cells were pre-treated with CA for 8 h followed by 6-OHDA treatment for an additional 16 h. We observed that while CA attenuates the 6-OHDA induced toxicity in SHSY5Y cells, its dose-dependent protective effect was abolished in NRF2 or hTERT silenced cells (Fig. 6 and Supplementary Fig. S6). These results suggest that both NRF2 and hTERT activation are essential for CA-dependent protection against 6-OHDA toxicity.

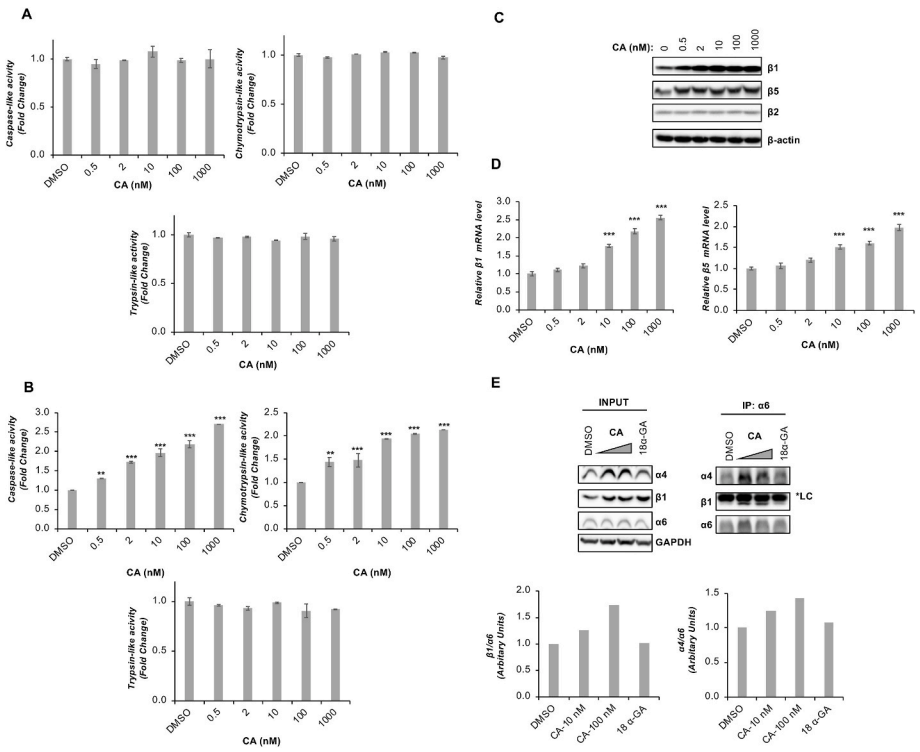

Fig. 3. The effect of CA on proteasome status. (A) Proteasome-enriched lysate of HEKn cells was incubated with indicated concentrations of CA. Proteasome subunits' activities were determined *via* fluorogenic substrates (n = 3; *p ≤ 0.05, **p ≤ 0.001, ***p ≤ 0.005). (B, C, D, E). HEKn cells were treated with the indicated concentration of CA for 24 h. (B) Fluorogenic substrates were used to evaluate the proteasome subunits' activities. The activity data were normalized to cellular total protein level and presented as a fold change compared to control cells treated with DMSO used as solvent control. Error bars are presented as standard deviations (n = 3; *p ≤ 0.05, **p ≤ 0.001, ***p ≤ 0.005). (C) The total protein levels of β1, β2, and β5 were evaluated by IB. β-actin was used as a loading control. (D) The mRNA levels of β1 and β5 were investigated by RT-qPCR. Error bars are presented as standard deviations (n = 3; *p ≤ 0.05, **p ≤ 0.001, ***p ≤ 0.005). (E) The effect of CA on the proteasome assembly was determined by IP. 18 α-GA (2 μg/ml; 4.25 μM) was used as an experimental control. After IP, the protein levels of α6, α4, and β1 were evaluated by IB using antibodies against them; *LC, light chain. GAPDH was used as a loading control for Input.

4. Discussion

Radix Astragali extract was found to have potential to improve population doubling time of human fetal lung diploid fibroblast and fetal kidney cells *in vitro* in the 1970s [59], and ingredients of the extract have been fully investigated to determine the compounds responsible for delaying senescence and having anti-aging effects as well as wound healing, and anti-inflammatory properties [60–62]. One of the major active compounds that are extracted from *Radix Astragalus membranaceus* is Astragaloside IV (AS-IV, 3-*O*-beta-D-xylopyranosyl, 6-*O*-beta-D-glucopyranosyl-cycloastragenol). In the literature, there are several studies showing that AS-IV protects cells against ROS [63], ischemia/reperfusion damages [64], lung injury [65], and cardiac hypertrophy [66] *via* NRF2 activation. The other major compound, CA, which is an aglycone and *in vivo* metabolite of AS-IV was discovered as a telomerase activator by TRAP (Telomere Repeat Amplification Protocol) assay [35]. Furthermore, CA has been implicated in the regulation of various cellular processes as comforting ER stress-related to inflammasome activation [37], improving autophagy *via* inhibition of AKT1-RPS6KB1 signaling [67], alleviating hepatic steatosis by activation of farnesoid X receptor signaling [68], activation of Src/MEK/ERK pathway [69] and upregulation of SIRT1 to prevent neuroinflammation in the ischemic brain [70]. Importantly, CA not only increases telomerase activity and elongates telomere length but also extends life span of mice without augmenting cancer incidences [33]. Furthermore, in clinical studies, CA (active ingredient of TA-65®) treatment showed no adverse effects but reduced blood sugar, insulin, total cholesterol, body mass index, and blood pressure [34]. The decrease in the ratio of total antioxidant capacity and 8-isoprostane levels, which is a hallmark for oxidative lipid damage, suggests that TA-65® may affect redox homeostasis.

All previous reports show that CA is a promising agent in the treatment of age-related diseases, but the molecular mechanisms for how CA influences aging-related main cellular processes such as telomerase activity, redox balance, and proteostasis have not been fully established. Previously, CA was suggested to ameliorate the decrease in NRF2 expression caused by TNF-α treatment in vascular smooth muscle cells. In another study, 50 μM CA slightly increased the NRF2 transcription in HepG2 cancer cells [71], which has much higher intrinsic telomerase expression compared to normal human cells [72,73]. In this study, we found that CA not only increased NRF2 protein expression but also enhanced the nuclear localization of NRF2, leading to ARE-promotor activity and consequently increasing the levels of cytoprotective enzymes such as HO-1, GR, and GCLC to protect cells against oxidative stress in human neonatal keratinocytes (Fig. 1).

CA is well-known as a telomerase activator, but its effect on hTERT levels and subcellular localization, as well as their underlying mechanisms, have not been elucidated. Here, in addition to potentiating hTERT expression, we have substantiated that CA increases the nuclear transport of hTERT (Fig. 2C). Several regulatory proteins play essential roles in the process of hTERT transport to the nucleus. The molecular chaperons p23 and Hsp90 are required to maintain an appropriate hTERT conformation that enables its nuclear translocation [51,52]. Moreover, the transport of hTERT along microtubules to the nucleus is facilitated by FKBP52, which links the hTERT–Hsp90 complex to the dynein–dynactin motor [48]. On the other hand, CHIP physically associates with hTERT in the cytosol and prevents its nuclear translocation by disassociating p23, suggesting that CHIP can remodel the hTERT-chaperone complexes. The resulting cytoplasmic hTERT is ubiquitinated by CHIP and subsequently degraded by the proteasome [49]. Our results revealed that CA enhanced the levels of proteins that function in the nuclear localization of hTERT while decreasing the expression of CHIP, which is known to prevent hTERT nuclear localization and increase hTERT degradation (Fig. 2D and E). Thus, our data suggest that CA not only increases the expression of hTERT but also enhances its nuclear localization through increasing the levels of Hsp90-based telomerase-associated chaperone complex and augmenting the interaction of hTERT with this complex to contribute to the telomerase activity (Fig. 2 A-F). The nuclear localization of hTERT is a critical process for the formation of catalytically active telomerase that functions on telomere maintenance. Interestingly, oxidative stress induces nuclear export of hTERT [55,74]. Moreover, upon H_2O_2 treatment, no degradation of hTERT protein was observed, but rather a concomitant increase within the mitochondria [55,74]. Supporting this

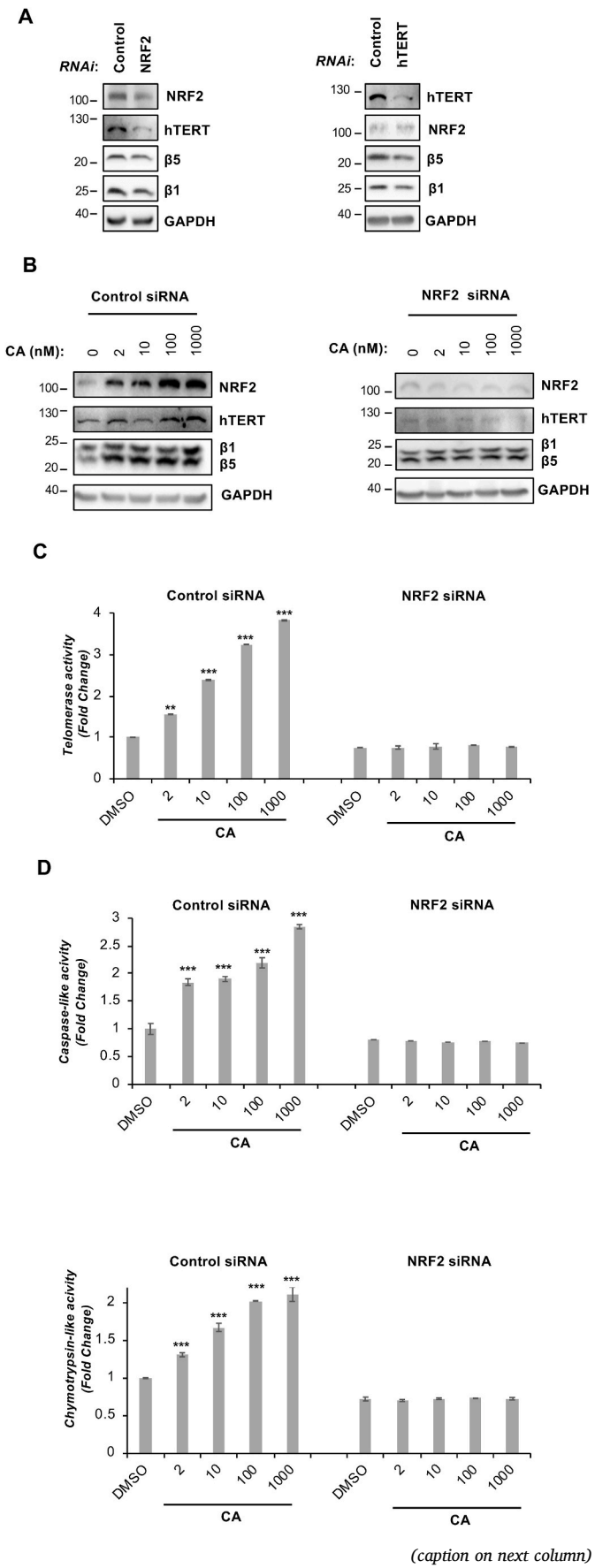

(caption on next column)

Fig. 4. The proteasomal activation of CA is mediated by NRF2. (A) HEKn cells were transfected with either oligo duplex specific to NRF2, hTERT, or Control siRNA. After 48 h later, cells were harvested, and total protein levels of hTERT, NRF2, β1, and β5 were determined by IB. GAPDH was used as a loading control. (B, C, D) HEKn cells were transfected with either NRF2 or Control siRNA (each of them 2 nM). After 48 h later, cells were treated with indicated concentrations of CA for 24 h. (B) The total protein levels of NRF2, hTERT, β1, and β5 were determined by IB. (C) The telomerase enzyme activity was determined by using ELISA (n:3, *p ≤ 0.05, **p ≤ 0.001, ***p ≤ 0.005). (D) The proteasomal β1 and β5 subunit activities were determined by using fluorogenic substrates. The activity data were normalized to cellular total protein level and presented as a fold change compared to control cells treated with DMSO used as a solvent control (n:3, *p ≤ 0.05, **p. ≤ 0.001, ***p ≤ 0.005).

view, we also observed that the mitochondrial hTERT levels increased upon H_2O_2 treatment (Fig. 2G). hTERT was found to be associated with mitochondrial DNA (mtDNA) as well as mitochondrial tRNA and localized in the mitochondrial matrix [75,76], where it should have non-telomeric functions as circular mtDNA does not contain telomeres. The function of hTERT in mitochondria has been controversially reported [54]. Aggravated mtDNA damage and apoptosis were reported in TERT-overexpressing fibroblast cell lines upon oxidative stress [77]. Conversely, it has also been demonstrated that TERT protects mtDNA and reduces mitochondrial ROS production suggesting a protective role for TERT in mitochondria [75]. When examining the effect of CA on the subcellular localization of hTERT in the presence of oxidative stress, we observed that CA attenuated the H_2O_2-induced mitochondrial hTERT levels. Furthermore, the nuclear hTERT level was increased with CA treatment compared to solvent control, even in the presence of oxidative stress (Fig. 2G). Additionally, CA diminished the mitochondrial ROS levels induced by H_20_2 (Fig. 2H). Considering the effect of CA to alleviate the H_2O_2-induced ROS production and its neuroprotective activities, it can be speculated that the reduction of mitochondrial hTERT and ROS levels by CA might be due to its cellular protective roles *via* NRF2/ARE against oxidative stress.

The proteasome genes are among the known-downstream targets of NRF2 pathway [78], and NRF2 increases proteasome subunit protein expression and proteasome activity [25,79]. Moreover, hTERT was determined to bind to multiple proteasome subunits and promote 26S proteasome assembly, which indicates another non-canonical function for hTERT that is independent of its telomere-regulatory function [80]. Studies toward the discovery of proteasome activators have been reported several natural and synthetic small compounds that stimulate proteasomal activity [81]. Although there are several studies regarding proteasome activation of triterpenoids such as Betulinic acid [82], 18α-GA [25], and Hederagenin [25], no study has been reported to determine the effects of CA on the proteasomal activity. As the regulation of proteasomal activity and/or assembly was found to be associated with both telomerase and NRF2 [25,56], the effect of CA on proteostasis was investigated. Here, we presented that CA not only enhances the activity of β1 and β5 proteasome subunits, responsible for caspase-like and chymotrypsin-like catalytic activities, respectively but also increases the mRNA/protein levels of these subunits and assembly of proteasome (Fig. 3B–E). With the results obtained from the present study, we propose that CA, known as a small molecule telomerase activator, would also be considered as a potent activator of NRF2 and proteasome.

In this study, we report for the first time that CA treatment affects multiple aging-related cellular processes such as hTERT, NRF2, and proteasome. In addition to the interrelationships of proteasome-hTERT and proteasome-NRF2 system, there are several studies about the bilateral relations between hTERT and NRF2. XRCC5 (X-ray repair cross-complementing 5), a transcriptional regulator factor binding to the hTERT promoter, was reported to physically interact with NRF2, which in turn upregulated hTERT in an NRF2 dependent manner in hepatocellular carcinoma (HCC) cells [83]. Consistently, administration of

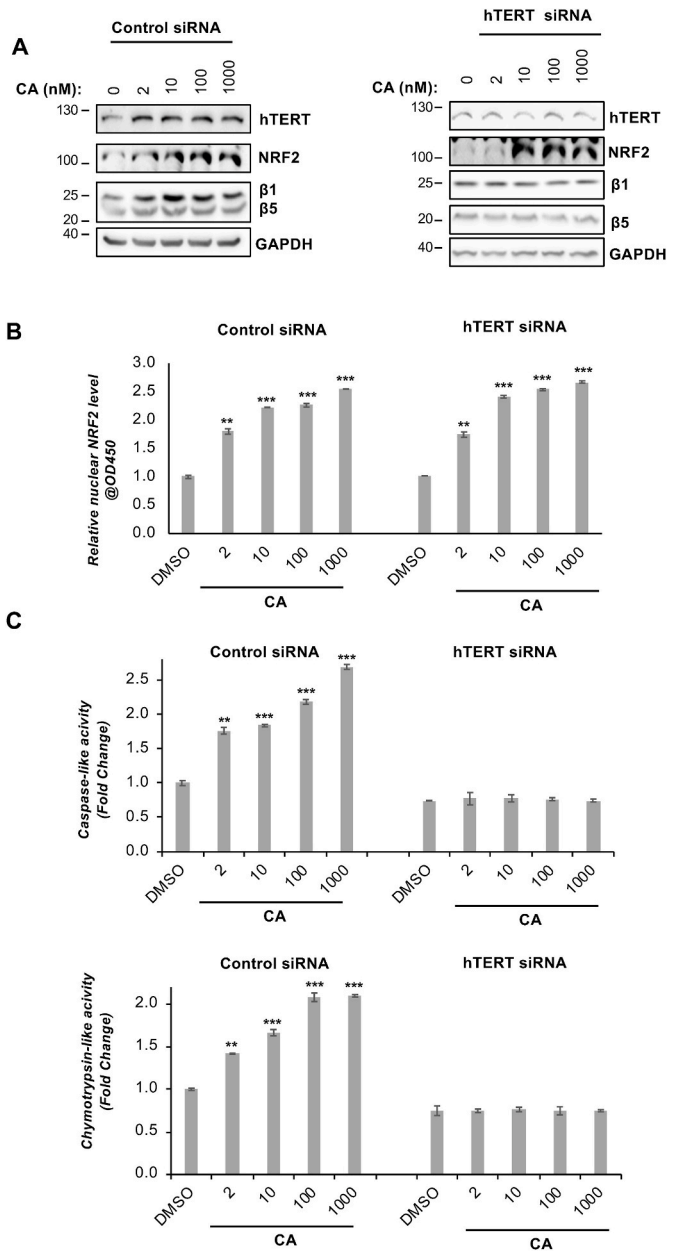

Fig. 5. The proteasomal activation of CA is also mediated by hTERT. HEKn cells were transfected with either oligo duplex specific to hTERT or Control siRNA. After 48 h later, cells were treated with CA for 24 h. (A) The total protein levels of NRF2, hTERT, β1, and β5 were determined by IB. (B) The NRF2 protein levels in nuclear fraction was determined by the NRF2 Transcription Factor Assay Kit and obtained data was normalized to nuclear protein level and presented as a fold change compared to control cells treated with DMSO used as solvent control. Error bars are presented as standard deviations (n = 3; *p ≤ 0.05, **p ≤ 0.001, ***p ≤ 0.005). (C) The proteasomal β1 and β5 subunit activities were evaluated *via* fluorogenic substrates. The data was normalized to cellular total protein level and presented as a fold change compared to control cells treated with DMSO used as solvent control. Error bars are presented as standard deviations ($n = 3$; *p ≤ 0.05, **p ≤ 0.001, ***p ≤ 0.005).

DMF, an activator of NRF2 pathway, to mice resulted in significant elevation of TERT mRNA levels [84]. TERT was also found significantly reduced in lung tissue of $Nrf2^{-/-}$ mice in the model of intestinal ischemia/reperfusion-induced acute lung injury [85]. On the other hand, hTERT G4-targeting small molecule (RG1603), or pharmacological inhibitor of hTERT (costunolide) and siRNA-mediated depletion of hTERT expression resulted in inhibition of NRF2 and HO-1 expression in

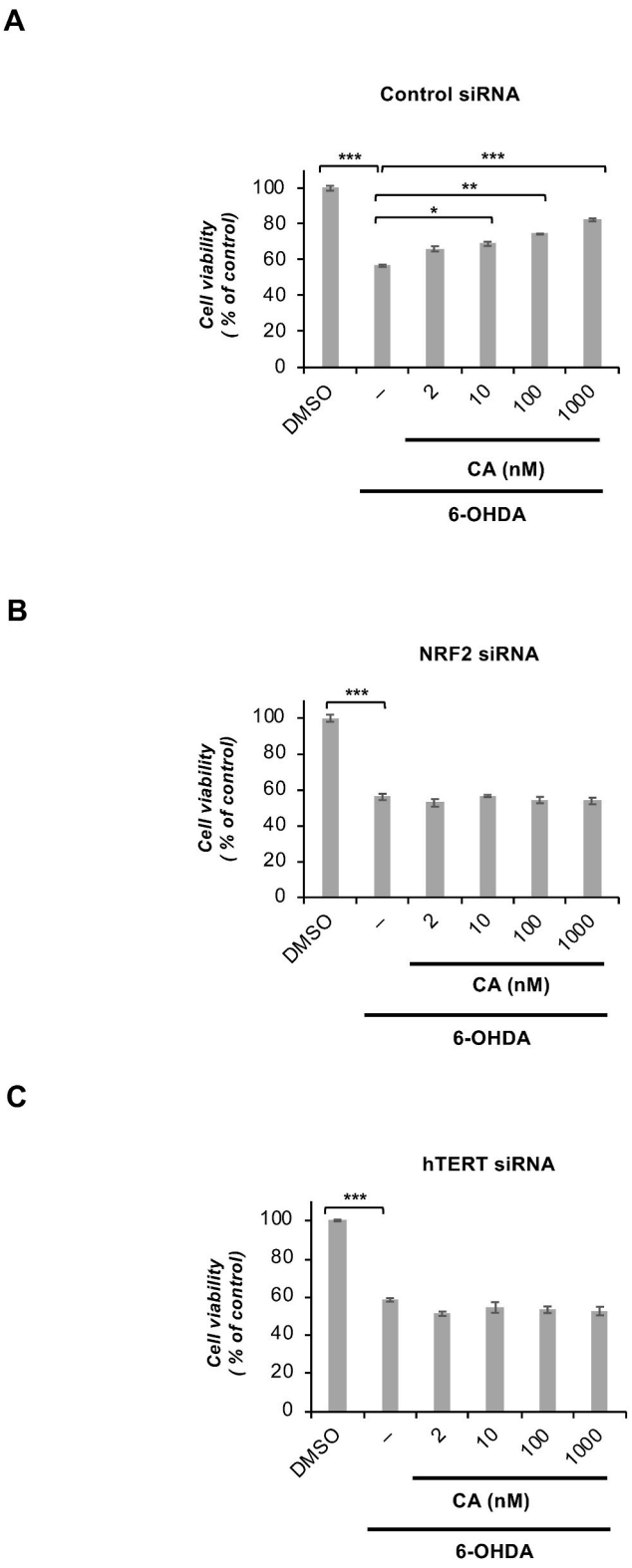

Fig. 6. The neuroprotection of CA against 6-OHDA is mediated by both NRF2 and hTERT. (A, B, C) HEKn cells were transfected with NRF2, hTERT, and Control siRNA. After 48 h later, cells were pre-treated with the desired concentration of CA for 8 h, then treated with 6-OHDA for 16 h. The cell viability was assessed by MTT reagent. The absorbance value of cells treated with DMSO as a solvent control for each experiment was considered 100%, and the viabilities of others were calculated. This assay was performed by triplicate samples. Student's t-test was used to determine the significance of the differences Error bars are presented as standard deviations (n = 3; *p ≤ 0.05, **p ≤ 0.001, ***p ≤ 0.005).

glioblastoma and prostate cancer [86,87]. Interestingly, hTERT was found to be primarily upregulated NRF2 by increasing NRF2 promoter activity rather than by regulating NRF2 mRNA or protein stability in colon cancer cells [88]. Considering our results, which revealed that CA increased both NRF2, telomerase, and proteasome activity, we aimed to identify the underlying mechanism in the next step. First, we found that NRF2 silencing caused downregulation of hTERT protein levels, but hTERT silencing had no significant effect on NRF2 protein levels (Fig. 4A). Second, we found that CA lost its ability to increase the protein levels and activities of hTERT, β1, and β5 proteasomal subunits in NRF2 silenced HEkn cells (Fig. 4B-D). On the other hand, in hTERT-silenced HEKn cells, CA still retained its ability to increase NRF2 activity but lost its effect on the proteasome (Fig. 5). Considering all these data together, it can be suggested that the telomerase activator effect of CA may be dependent on NRF2 activity or due to the significant decrease in hTERT expression observed in NRF2 silenced cells, CA cannot be able to increase the telomerase activity in NRF2 silenced cells.

CA treatment exhibited stimulatory effect on telomerase activity, which was consistent with augmented TERT expression and nuclear translocation. Additionally, CA robustly augmented expression of ARE signaling molecules, including NRF2, HO-1, GR, and GCLC. Thus, CA could antagonize oxidative/electrophilic stress and DNA damage while improving telomere function, which are known to be important in neurodegenerative diseases. On the other hand, neurodegenerative diseases such as Parkinson's, Alzheimer's, and Huntington's have been associated with intracellular ubiquitin-positive inclusions formed by aggregate-prone neurotoxic proteins. It has been reported that the aberrant ubiquitin-proteasome system in neurodegenerative diseases contributes to the accumulation of neurotoxic proteins that perturb cellular homeostasis and neuronal function and to instigate neurodegeneration [6,59,89]. Thus, enhancement of proteasome activity by small molecules has been considered as a new approach for treatment of neurodegenerative diseases [60]. Based on the data observed from this study suggesting that CA potently activates proteasome through activation of hTERT and NRF2 systems, we analyzed the molecular mechanism of reported neuroprotection properties [58,90] of CA by utilizing 6-OHDA toxicity in NRF2 and hTERT silenced HEKn cells. While CA provided neuroprotection against 6-OHDA in a dose-dependent manner, this neuroprotection was abolished in both hTERT, and NRF2 silenced HEKn cells suggesting that the neuroprotective effect of CA is driven by these pathways (Fig. 6).

Our results provide new evidence for the cross-talk among NRF2, telomerase, and proteasome systems, as well as for the molecular mechanism by which CA acts at the intersection of these three aging-related cellular processes (Fig. 7) further indicating that the potential of CA as preventive and/or therapeutic molecule against physiological and pathophysiological conditions associated with oxidative stress, telomere attrition, and loss of proteostasis.

Author contributions

P·B·K and E.B. conceived the *hypotheses* and designed the study. S.Y. participated in the design of the experiments, conducted the experiments, and collected the data. P.B.K, E.B and S.Y. analyzed the results and contributed to the manuscript preparation. All authors read and approved the manuscript.

Funding

This study was supported by Scientific and Technological Research Council of Turkey (TUBITAK, Grant number: 119Z086).

Data statement availability

The data that support the findings of this study are available from the corresponding author upon request.

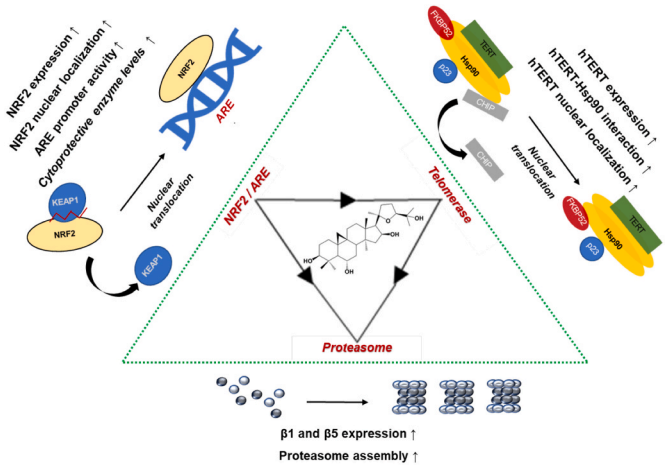

Fig. 7. The schematic illustration of the molecular mechanism of CA activity. CA increases NRF2 activity leading to upregulation of cytoprotective enzymes. CA also enhances telomerase activity by increasing not only the expression of hTERT but also its nuclear localization *via* the Hsp90-chaperon complex. The proteasome activity and assembly are increased by the treatment of CA, that is dependent on induction of telomerase activity, which is mediated by NRF2 system.

Declaration of competing interest

The authors declare that there is no conflict of interest.

Acknowledgments

We thank the Pharmaceutical Sciences Research Centre (FABAL, Ege University, Faculty of Pharmacy) for equipment support and Bionorm Natural Products for donating CA. We also thank to Sermin Genc from Izmir International Biomedicine and Genome Institute (iBG-Izmir) for providing MitoSOX.

Appendix A. Supplementary data

Supplementary data to this article can be found online at https://doi.org/10.1016/j.freeradbiomed.2022.06.230.

References

[1] C. Lopez-Otin, M.A. Blasco, L. Partridge, M. Serrano, G. Kroemer, The hallmarks of aging, Cell 153 (6) (2013) 1194–1217.
[2] A.B. Salmon, A. Richardson, V.I. Perez, Update on the oxidative stress theory of aging: does oxidative stress play a role in aging or healthy aging? Free Radical Biol Med. 48 (5) (2010) 642–655.
[3] C.J. Schmidlin, M.B. Dodson, L. Madhavan, D.D. Zhang, Redox regulation by NRF2 in aging and disease, Free Radical Biol Med. 134 (2019) 702–707.
[4] H.Q. Zhang, K.J.A. Davies, H.J. Forman, Oxidative stress response and Nrf2 signaling in aging, Free Radical Biol Med. 88 (2015) 314–336.
[5] H. Zhang, K.J.A. Davies, H.J. Forman, Oxidative stress response and Nrf2 signaling in aging, Free Radical Biol Med. 88 (Pt B) (2015) 314–336.
[6] D.D. Zhang, M. Hannink, Distinct cysteine residues in Keap1 are required for Keap1-dependent ubiquitination of Nrf2 and for stabilization of Nrf2 by chemopreventive agents and oxidative stress, Mol. Cell Biol. 23 (22) (2003) 8137–8151.
[7] K. Yoh, K. Itoh, A. Enomoto, A. Hirayama, N. Yamaguchi, M. Kobayashi, N. Morito, A. Koyama, M. Yamamoto, S. Takahashi, Nrf2-deficient female mice develop lupus-like autoimmune nephritis, Kidney Int. 60 (4) (2001) 1343–1353.
[8] S.S. Gounder, S. Kannan, D. Devadoss, C.J. Miller, K.S. Whitehead, S.J. Odelberg, M.A. Firpo, R. Paine, J.R. Hoidal, E.D. Abel, N.S. Rajasekaran, Impaired transcriptional activity of Nrf2 in age-related myocardial oxidative stress is reversible by moderate exercise training, PLoS One. 7 (9) (2012).
[9] L. Hecker, N.J. Logsdon, D. Kurundkar, A. Kurundkar, K. Bernard, T. Hock, E. Meldrum, Y.Y. Sanders, V.J. Thannickal, Reversal of persistent fibrosis in aging by targeting nox4-nrf2 redox imbalance, Sci. Transl. Med. 6 (231) (2014).
[10] M. Narasimhan, J. Hong, N. Atieno, V.R. Muthusamy, C.J. Davidson, N. Abu-Rmaileh, R.S. Richardson, A.V. Gomes, J.R. Hoidal, N.S. Rajasekaran, Nrf2

deficiency promotes apoptosis and impairs PAX7/MyoD expression in aging skeletal muscle cells, Free Radical Bio Med. 71 (2014) 402–414.
[11] S. Tarantini, M.N. Valcarcel-Ares, A. Yabluchanskiy, Z. Tucsek, P. Hertelendy, T. Kiss, T. Gautam, X.A. Zhang, W.E. Sonntag, R. de Cabo, E. Farkas, M.H. Elliott, M.T. Kinter, F. Deak, Z. Ungvari, A. Csiszar, Nrf2 deficiency exacerbates obesity-induced oxidative stress, neurovascular dysfunction, blood-brain barrier disruption, neuroinflammation, amyloidogenic gene expression, and cognitive decline in mice, mimicking the aging phenotype, J Gerontol a-Biol. 73 (7) (2018) 853–863.
[12] G.A. Fulop, T. Kiss, S. Tarantini, P. Balasubramanian, A. Yabluchanskiy, E. Farkas, F. Bari, Z. Ungvari, A. Csiszar, Nrf2 deficiency in aged mice exacerbates cellular senescence promoting cerebrovascular inflammation, Geroscience 40 (5–6) (2018) 513–521.
[13] B. Ahn, G. Pharaoh, P. Premkumar, K. Huseman, R. Ranjit, M. Kinter, L. Szweda, T. Kiss, G. Fulop, S. Tarantini, A. Csiszar, Z. Ungvari, H. Van Remmen, Nrf2 deficiency exacerbates age-related contractile dysfunction and loss of skeletal muscle mass, Redox Biol. 17 (2018) 47–58.
[14] M.N. Valcarcel-Ares, S. Tarantini, P. Hertelendy, Z. Tucsek, T. Gautam, T. Kiss, R. De Cabo, E. Farkas, M. Kinter, W.E. Sonntag, A. Csiszar, Z. Ungvari, Interaction of obesity and Nrf2 deficiency accelerates cerebromicrovascular aging and impairs neurovascular coupling responses, Faseb. J. 31 (2017).
[15] S.J. Chapple, R.C. Siow, G.E. Mann, Crosstalk between Nrf2 and the proteasome: therapeutic potential of Nrf2 inducers in vascular disease and aging, Int. J. Biochem. Cell Biol. 44 (8) (2012) 1315–1320.
[16] I. Saez, D. Vilchez, The mechanistic links between proteasome activity, aging and agerelated diseases, Curr. Genom. 15 (1) (2014) 38–51.
[17] G. Ben-Nissan, M. Sharon, Regulating the 20S proteasome ubiquitin-independent degradation pathway, Biomolecules 4 (3) (2014) 862–884.
[18] J.M. Baugh, E.G. Viktorova, E.V. Pilipenko, Proteasomes can degrade a significant proportion of cellular proteins independent of ubiquitination, J. Mol. Biol. 386 (3) (2009) 814–827.
[19] V. Andersson, S. Hanzen, B. Liu, M. Molin, T. Nystrom, Enhancing protein disaggregation restores proteasome activity in aged cells, Aging (Albany NY) 5 (11) (2013) 802–812.
[20] N. Chondrogianni, K. Voutetakis, M. Kapetanou, V. Delitsikou, N. Papaevgeniou, M. Sakellari, M. Lefaki, K. Filippopoulou, E.S. Gonos, Proteasome activation: an innovative promising approach for delaying aging and retarding age-related diseases, Ageing Res. Rev. 23 (Pt A) (2015) 37–55.
[21] E. Bellavista, M. Martucci, F. Vasuri, A. Santoro, M. Mishto, A. Kloss, E. Capizzi, A. Degiovanni, C. Lanzarini, D. Remondini, A. Dazzi, S. Pellegrini, M. Cescon, M. Capri, S. Salvioli, A. D'Errico-Grigioni, B. Dahlmann, G.L. Grazi, C. Franceschi, Lifelong maintenance of composition, function and cellular/subcellular distribution of proteasomes in human liver, Mech. Ageing Dev. 141 (2014) 26–34.
[22] N. Chondrogianni, M. Sakellari, M. Lefaki, N. Papaevgeniou, E.S. Gonos, Proteasome activation delays aging in vitro and in vivo, Free Radic. Biol. Med. 71 (2014) 303–320.
[23] D. Vilchez, I. Saez, A. Dillin, The role of protein clearance mechanisms in organismal ageing and age-related diseases, Nat. Commun. 5 (2014).
[24] N. Chondrogianni, C. Tzavelas, A.J. Pemberton, I.P. Nezis, A.J. Rivett, E.S. Gonos, Overexpression of proteasome beta5 assembled subunit increases the amount of proteasome and confers ameliorated response to oxidative stress and higher survival rates, J. Biol. Chem. 280 (12) (2005) 11840–11850.
[25] S. Kapeta, N. Chondrogianni, E.S. Gonos, Nuclear erythroid factor 2-mediated proteasome activation delays senescence in human fibroblasts, J. Biol. Chem. 285 (11) (2010) 8171–8184.
[26] C.W. Greider, Telomere length regulation, Annu. Rev. Biochem. 65 (1996) 337–365.
[27] E.H. Blackburn, Structure and function of telomeres, Nature 350 (6319) (1991) 569–573.
[28] G.D. Richardson, D. Breault, G. Horrocks, S. Cormack, N. Hole, A. Owens, Telomerase expression in the mammalian heart, Faseb. J. 26 (12) (2012) 4832–4840.
[29] M. Zurek, J. Altschmied, S. Kohlgruber, N. Ale-Agha, J. Haendeler, Role of telomerase in the cardiovascular system, Genes-Basel 7 (6) (2016).
[30] F. Iannilli, F. Zalfa, A. Gartner, C. Bagni, C.G. Dotti, Cytoplasmic TERT associates to RNA granules in fully mature neurons: role in the translational control of the cell cycle inhibitor p15INK4B, PLoS One. 8 (6) (2013).
[31] A. Spilsbury, S. Miwa, J. Attems, G. Saretzki, The role of telomerase protein TERT in alzheimer's disease and in tau-related pathology in vitro, J. Neurosci. 35 (4) (2015) 1659–1674.
[32] E. Segal-Bendirdjian, V. Geli, Non-canonical roles of telomerase: unraveling the imbroglio, Front. Cell Dev. Biol. 7 (2019) 332.
[33] B. Bernardes de Jesus, K. Schneeberger, E. Vera, A. Tejera, C.B. Harley, M. A. Blasco, The telomerase activator TA-65 elongates short telomeres and increases health span of adult/old mice without increasing cancer incidence, Aging Cell 10 (4) (2011) 604–621.
[34] C.B. Harley, W. Liu, P.L. Flom, J.M. Raffaele, A natural product telomerase activator as part of a health maintenance program: metabolic and cardiovascular response, Rejuvenation Res. 16 (5) (2013) 386–395.
[35] F.C.F. Ip, Y.P. Ng, H.J. An, Y. Dai, H.H. Pang, Y.Q. Hu, A.C. Chin, C.B. Harley, Y. H. Wong, N.Y. Ip, Cycloastragenol is a potent telomerase activator in neuronal cells: implications for depression management, Neurosignals 22 (1) (2014) 52–63.
[36] C.T. Dow, C.B. Harley, Evaluation of an oral telomerase activator for early age-related macular degeneration - a pilot study, Clin. Ophthalmol. 10 (2016) 243–249.
[37] Y. Zhao, Q. Li, W. Zhao, J. Li, Y. Sun, K. Liu, B. Liu, N. Zhang, Astragaloside IV and cycloastragenol are equally effective in inhibition of endoplasmic reticulum stress-associated TXNIP/NLRP3 inflammasome activation in the endothelium, J. Ethnopharmacol. 169 (2015) 210–218.
[38] S. Hummasti, G.S. Hotamisligil, Endoplasmic reticulum stress and inflammation in obesity and diabetes, Circ. Res. 107 (5) (2010) 579–591.
[39] P. Libby, Y. Okamoto, V.Z. Rocha, E. Folco, Inflammation in atherosclerosis: transition from theory to practice, Circ. J. 74 (2) (2010) 213–220.
[40] I. Stasik, A. Rapak, E. Ziolo, L. Strzadala, The mitochondrial localization of RelB and NFATx in immature T cells, Cell. Mol. Biol. Lett. 13 (4) (2008) 493–501.
[41] G. Uner, O. Tag, Y. Erzurumlu, P.B. Kirmizibayrak, E. Bedir, Identification of a noncanonical necrotic cell death triggered via enhanced proteolysis by a novel sapogenol derivative, Chem. Res. Toxicol. 33 (11) (2020) 2880–2891.
[42] B. Karademir, G. Sari, A.T. Jannuzzi, S. Musunuri, G. Wicher, T. Grune, J. Mi, H. Hacioglu-Bay, K. Forsberg-Nilsson, J. Bergquist, T. Jung, Proteomic approach for understanding milder neurotoxicity of Carfilzomib against Bortezomib, Sci Rep-Uk 8 (2018).
[43] E. Gezer, G. Uner, M. Kucuksolak, M.U. Kurt, G. Dogan, P.B. Kirmizibayrak, E. Bedir, Undescribed polyether ionophores from Streptomyces cacaoi and their antibacterial and antiproliferative activities, Phytochemistry 195 (2022), 113038.
[44] B. Tastan, B.I. Arioz, K.U. Tufekci, E. Tarakcioglu, C.P. Gonul, K. Genc, S. Genc, Dimethyl fumarate alleviates NLRP3 inflammasome activation in microglia and sickness behavior in LPS-challenged mice, Front. Immunol. 12 (2021).
[45] L.W. Hu, J.H. Yen, Y.T. Shen, K.Y. Wu, M.J. Wu, Luteolin modulates 6-hydroxy-dopamine-induced transcriptional changes of stress response pathways in PC12 cells, PLoS One. 9 (5) (2014), e97880.
[46] Y. Cao, L. Xu, X. Yang, Y. Dong, H. Luo, F. Xing, Q. Ge, The potential role of cycloastragenol in promoting diabetic wound repair in vitro, BioMed Res. Int. 2019 (2019), 7023950.
[47] J.H. Wu, Z.W. Zeng, Y.Y. Li, H.Y. Qin, C.Q. Zuo, C.H. Zhou, D.H. Xu, Cycloastragenol protects against glucocorticoid-induced osteogenic differentiation inhibition by activating telomerase, Phytother Res. 35 (4) (2021) 2034–2044.
[48] Y.Y. Jeong, J. Her, S.Y. Oh, I.K. Chung, Hsp90-binding immunophilin FKBP52 modulates telomerase activity by promoting the cytoplasmic retrotransport of hTERT, Biochem. J. 473 (2016) 3517–3532.
[49] J.H. Lee, P. Khadka, S.H. Baek, I.K. Chung, CHIP promotes human telomerase reverse transcriptase degradation and negatively regulates telomerase activity, J. Biol. Chem. 285 (53) (2010) 42033–42045.
[50] J.H. Kim, S.M. Park, M.R. Kang, S.Y. Oh, T.H. Lee, M.T. Muller, I.K. Chung, Ubiquitin ligase MKRN1 modulates telomere length homeostasis through a proteolysis of hTERT, Gene Dev. 19 (7) (2005) 776–781.
[51] S.E. Holt, D.L. Aisner, J. Baur, V.M. Tesmer, M. Dy, M. Ouellette, J.B. Trager, G. B. Morin, D.O. Toft, J.W. Shay, W.E. Wright, M.A. White, Functional requirement of p23 and Hsp90 in telomerase complexes, Gene Dev. 13 (7) (1999) 817–826.
[52] H.L. Forsythe, J.L. Jarvis, J.W. Turner, L.W. Elmore, S.E. Holt, Stable association of hsp90 and p23, but not hsp70, with active human telomerase, J. Biol. Chem. 276 (19) (2001) 15571–15574.
[53] S.A. Jeong, K. Kim, J.H. Lee, J.S. Cha, P. Khadka, H.S. Cho, I.K. Chung, Akt-mediated phosphorylation increases the binding affinity of hTERT for importin alpha to promote nuclear translocation (vol 128, pg 2287, 2015), J. Cell Sci. 128 (15) (2015), 2951-2951.
[54] J. Rosen, P. Jakobs, N. Ale-Agha, J. Altschmied, J. Haendeler, Non-canonical functions of telomerase reverse transcriptase - impact on redox homeostasis, Redox Biol. 34 (2020).
[55] J. Haendeler, J. Hoffmann, R.P. Brandes, A.M. Zeiher, S. Dimmeler, Hydrogen peroxide triggers nuclear export of telomerase reverse transcriptase via Src kinase family-dependent phosphorylation of tyrosine 707, Mol. Cell Biol. 23 (13) (2003) 4598–4610.
[56] J. Imai, M. Maruya, H. Yashiroda, I. Yahara, K. Tanaka, The molecular chaperone Hsp90 plays a role in the assembly and maintenance of the 26S proteasome, EMBO J. 22 (14) (2003) 3557–3567.
[57] M. Ikram, M.H. Jo, K. Choe, A. Khan, S. Ahmad, K. Saeed, M.W. Kim, M.O. Kim, Cycloastragenol, a triterpenoid saponin, regulates oxidative stress, neurotrophic dysfunctions, neuroinflammation and apoptotic cell death in neurodegenerative conditions, Cells-Basel 10 (10) (2021).
[58] T. Nesil, T. Nesil, A.S. Urkmez, E. Bedir, Protective effects of astragaloside IV and cycloastragenol in 6-hydroxydopamin (6-OHDA)-induced neurotoxicity in PC12 cells, Planta Med. 77 (12) (2011), 1444-1444.
[59] P.C. Wang, Z.Y. Zhang, Z. Ran, T.J. Tong, Two isomers of HDTIC isolated from Astragali Radix decrease the expression of p16 in 2BS cells, Chinese Med J-Peking 121 (3) (2008) 231–235.
[60] C. Sevimli-Gur, I. Onbasilar, P. Atilla, R. Genc, N. Cakar, I. Deliloglu-Gurhan, E. Bedir, In vitro growth stimulatory and in vivo wound healing studies on cycloartane-type saponins of Astragalus genus, J. Ethnopharmacol. 134 (3) (2011) 844–850.
[61] B.B. de Jesus, K. Schneeberger, E. Vera, A. Tejera, C.B. Harley, M.A. Blasco, The telomerase activator TA-65 elongates short telomeres and increases health span of adult/old mice without increasing cancer incidence, Aging Cell 10 (4) (2011) 604–621.
[62] E. Yesilada, E. Bedir, I. Calis, Y. Takaishi, Y. Ohmoto, Effects of triterpene saponins from Astragalus species on in vitro cytokine release, J. Ethnopharmacol. 96 (1–2) (2005) 71–77.
[63] H. Li, P. Wang, F. Huang, J. Jin, H. Wu, B. Zhang, Z. Wang, H. Shi, X. Wu, Astragaloside IV protects blood-brain barrier integrity from LPS-induced disruption via activating Nrf2 antioxidant signaling pathway in mice, Toxicol. Appl. Pharmacol. 340 (2018) 58–66.

[64] D.M. Gu, P.H. Lu, K. Zhang, X. Wang, M. Sun, G.Q. Chen, Q. Wang, EGFR mediates astragaloside IV-induced Nrf2 activation to protect cortical neurons against in vitro ischemia/reperfusion damages, Biochem Bioph Res Co 457 (3) (2015) 391–397.
[65] Z. Zhang, X. Cheng, D. Ge, S. Wang, B. Qi, Protective effects of astragaloside IV combined with budesonide in bronchitis in rats by regulation of nNrf2/Keap1 pathway, Med. Sci. Mon. Int. Med. J. Exp. Clin. Res. 24 (2018) 8481–8488.
[66] P. Nie, F.J. Meng, J.G. Zhang, X.Q. Wei, C. Shen, Astragaloside IV exerts a myocardial protective effect against cardiac hypertrophy in rats, partially via activating the Nrf2/HO-1 signaling pathway, Oxid. Med. Cell. Longev. 2019 (2019).
[67] J. Wang, M.L. Wu, S.P. Cao, H. Cai, Z.M. Zhao, Y.H. Song, Cycloastragenol ameliorates experimental heart damage in rats by promoting myocardial autophagy via inhibition of AKT1-RPS6KB1 signaling, Biomed. Pharmacother. 107 (2018) 1074–1081.
[68] M. Gu, S. Zhang, Y. Zhao, J. Huang, Y. Wang, Y. Li, S. Fan, L. Yang, G. Ji, Q. Tong, C. Huang, Cycloastragenol improves hepatic steatosis by activating farnesoid X receptor signalling, Pharmacol. Res. 121 (2017) 22–32.
[69] L.Y. Yung, W.S. Lam, M.K. Ho, Y. Hu, F.C. Ip, H. Pang, A.C. Chin, C.B. Harley, N. Y. Ip, Y.H. Wong, Astragaloside IV and cycloastragenol stimulate the phosphorylation of extracellular signal-regulated protein kinase in multiple cell types, Planta Med. 78 (2) (2012) 115–121.
[70] M. Li, S.C. Li, B.K. Dou, Y.X. Zou, H.Z. Han, D.X. Liu, Z.J. Ke, Z.F. Wang, Cycloastragenol upregulates SIRT1 expression, attenuates apoptosis and suppresses neuroinflammation after brain ischemia, Acta Pharmacol. Sin. 41 (8) (2020) 1025–1032.
[71] L.M. Feng, S. Ji, X. Qiao, Z.W. Li, X.H. Lin, M. Ye, Biocatalysis of cycloastragenol by syncephalastrum racemosum and Alternaria alternata to discover anti-aging derivatives, Adv. Synth. Catal. 357 (8) (2015) 1928–1940.
[72] M. Sakaguchi, T. Sadahira, H. Ueki, R. Kinoshita, H. Murata, K.I. Yamamoto, J. Futami, Y. Nasu, K. Ochiai, H. Kumon, N.H. Huh, M. Watanabe, Robust cancer-specific gene expression by a novel cassette with hTERT and CMV promoter elements, Oncol. Rep. 38 (2) (2017) 1108–1114.
[73] M. Watanabe, H. Ueki, K. Ochiai, P. Huang, Y. Kobayashi, Y. Nasu, K. Sasaki, H. Kaku, Y. Kashiwakura, H. Kumon, Advanced two-step transcriptional amplification as a novel method for cancer-specific gene expression and imaging, Oncol. Rep. 26 (4) (2011) 769–775.
[74] S. Ahmed, J.F. Passos, M.J. Birket, T. Beckmann, S. Brings, H. Peters, M.A. Birch-Machin, T. von Zglinicki, G. Saretzki, Telomerase does not counteract telomere shortening but protects mitochondrial function under oxidative stress, J. Cell Sci. 121 (Pt 7) (2008) 1046–1053.
[75] J. Haendeler, S. Drose, N. Buchner, S. Jakob, J. Altschmied, C. Goy, I. Spyridopoulos, A.M. Zeiher, U. Brandt, S. Dimmeler, Mitochondrial telomerase reverse transcriptase binds to and protects mitochondrial DNA and function from damage, Arterioscler. Thromb. Vasc. Biol. 29 (6) (2009) 929–935.
[76] N.K. Sharma, A. Reyes, P. Green, M.J. Caron, M.G. Bonini, D.M. Gordon, I.J. Holt, J.H. Santos, Human telomerase acts as a hTR-independent reverse transcriptase in mitochondria, Nucleic Acids Res. 40 (2) (2012) 712–725.
[77] J.H. Santos, J.N. Meyer, B. Van Houten, Mitochondrial localization of telomerase as a determinant for hydrogen peroxide-induced mitochondrial DNA damage and apoptosis, Hum. Mol. Genet. 15 (11) (2006) 1757–1768.
[78] M.K. Kwak, N. Wakabayashi, J.L. Greenlaw, M. Yamamoto, T.W. Kensler, Antioxidants enhance mammalian proteasome expression through the Keap1-Nrf2 signaling pathway, Mol. Cell Biol. 23 (23) (2003) 8786–8794.
[79] A. Arlt, I. Bauer, C. Schafmayer, J. Tepel, S.S. Muerkoster, M. Brosch, C. Roder, H. Kalthoff, J. Hampe, M.P. Moyer, U.R. Folsch, H. Schafer, Increased proteasome subunit protein expression and proteasome activity in colon cancer relate to an enhanced activation of nuclear factor E2-related factor 2 (Nrf2), Oncogene 28 (45) (2009) 3983–3996.
[80] E. Im, J.B. Yoon, H.W. Lee, K.C. Chung, Human telomerase reverse transcriptase (hTERT) positively regulates 26S proteasome activity, J. Cell. Physiol. 232 (8) (2017) 2083–2093.
[81] N. Chondrogianni, M.A. Vasilopoulou, M. Kapetanou, E.S. Gonos, Proteasome modulation: a way to delay aging? Encyclopedia of Biomedical Gerontology 3 (2020) 92–104.
[82] L. Huang, P. Ho, C.H. Chen, Activation and inhibition of the proteasome by betulinic acid and its derivatives, FEBS Lett. 581 (25) (2007) 4955–4959.
[83] T. Liu, Q. Long, L. Li, H. Gan, X. Hu, H. Long, L. Yang, P. Pang, S. Wang, W. Deng, The NRF2-dependent transcriptional axis, XRCC5/hTERT drives tumor progression and 5-Fu insensitivity in hepatocellular carcinoma, Molecular Therapy - Oncolytics 24 (2022) 249–261.
[84] N. Akino, O. Wada-Hiraike, W. Isono, H. Terao, H. Honjo, Y. Miyamoto, M. Tanikawa, K. Sone, M. Hirano, M. Harada, T. Hirata, Y. Hirota, K. Koga, K. Oda, T. Fujii, Y. Osuga, Activation of Nrf2/Keap1 pathway by oral Dimethylfumarate administration alleviates oxidative stress and age-associated infertility might be delayed in the mouse ovary, Reprod. Biol. Endocrinol. 17 (1) (2019) 23.
[85] H. Dong, Y. Xia, S. Jin, C. Xue, Y. Wang, R. Hu, H. Jiang, Nrf2 attenuates ferroptosis-mediated IIR-ALI by modulating TERT and SLC7A11, Cell Death Dis. 12 (11) (2021) 1027.
[86] J.H. Song, H.J. Kang, L.A. Luevano, V. Gokhale, K. Wu, R. Pandey, H.H. Sherry Chow, L.H. Hurley, A.S. Kraft, Small-molecule-targeting hairpin loop of hTERT promoter G-quadruplex induces cancer cell death, Cell Chemical Biology. 26 (8) (2019) 1110–1121 e4.
[87] F. Ahmad, D. Dixit, V. Sharma, A. Kumar, S.D. Joshi, C. Sarkar, E. Sen, Nrf2-driven TERT regulates pentose phosphate pathway in glioblastoma, Cell Death Dis. 7 (2016) e2213.
[88] C. Gong, H. Yang, S. Wang, J. Liu, Z. Li, Y. Hu, Y. Chen, Y. Huang, Q. Luo, Y. Wu, E. Liu, Y. Xiao, hTERT promotes CRC proliferation and migration by recruiting YBX1 to increase NRF2 expression, Front. Cell Dev. Biol. 9 (2021), 658101.
[89] Q. Zheng, T. Huang, L. Zhang, Y. Zhou, H. Luo, H. Xu, X. Wang, Dysregulation of ubiquitin-proteasome system in neurodegenerative diseases, Front. Aging Neurosci. 8 (2016) 303.
[90] T. Wan, E.J. Weir, M. Johnson, V.I. Korolchuk, G.C. Saretzki, Increased telomerase improves motor function and alpha-synuclein pathology in a transgenic mouse model of Parkinson's disease associated with enhanced autophagy, Prog. Neurobiol. 199 (2021), 101953.